AIAA Journal
Vol. 40, No. 8, August 2002

Technical Notes

TECHNICAL NOTES are short manuscripts describing new developments or important results of a preliminary nature. These Notes cannot exceed six manuscript pages and three figures; a page of text may be substituted for a figure and vice versa. After informal review by the editors, they may be published within a few months of the date of receipt. Style requirements are the same as for regular contributions (see inside back cover).

Motion of Variable Geometry Truss for Momentum Management in Spacecraft

Kazuyuki Hanahara* and Yukio Tada†
Kobe University, Kobe 657-8501, Japan

Introduction

A MULTIUNIT orbital platform system is a promising candidate for future space missions. It is a concept of an artificial satellite system designed for a number of different mission units sharing such as power and communication facilities. Compared with conventional single-unit satellites, this kind of platform system is considered to have the following two advantages. One is reduction of total payload to be launched. The other is more effective use of orbital space, that is, the increase in number of satellites can be relieved by means of the platform systems and it is helpful to avoid collision among satellites, especially in the geostationary orbit, where many satellites have already been in operation. The multiunit platform system is, however, considered to have the problem of interference among the mission units especially as a result of the law of conservation of momentum. For example, if an observation unit on a platform changes the direction of its optical equipment, the direction of an optical equipment of another unit on the same platform can be affected.

In this Note, the idea of an adaptive structure[1] is studied to cope with this problem. The mission units having movable parts are installed through the variable geometry truss (VGT)[2] so that the momentum interference caused by the movable parts is reduced by the VGT motion. The conceptual sketch of the proposed approach is shown in Fig. 1; mission units having movable parts are installed at the peripheral ends of VGTs on the platform. This type of installation of mission unit is considered to have another advantage that it can help adjust the position and orientation of the mission unit. Formulation of coordinate transformation of linear and angular momentum between the local coordinate of mission unit at the peripheral end of VGT and the global coordinate of the platform is discussed because the Euler's equation is not convenient for the angular momentum of a mission unit that has movable parts, in the case of coordinate transformation with translation as well as rotation. The motion planning problem of VGT to reduce the momentum interference is formulated based on the coordinate transformation. Computer simulation is carried out, and the effect of momentum interference reduction is demonstrated.

Coordinate Transformation of Linear and Angular Momentum

The simplest way to deal with a number of values of linear and angular momentum is to calculate all of the values referring to the same global coordinate from the beginning of the formulation. This kind of approach is not suitable for a multiunit system because a task to be performed in one unit is often described in a local coordinate. Coordinate transformation of angular momentum convenient for a mission unit having movable parts, however, has not been seen to date as far as the authors know. The conventional Euler's equation is not appropriate in this case because it requires the values of linear and angular momentum of all individual rigid bodies of the mission unit in order to evaluate the total momentum in the global coordinate. We introduce a formulation of coordinate transformation of linear and angular momentum suitable to the situation, which does not need momentum values of individual rigid bodies of the mission unit.

Basic Equation

The basic equation of coordinate transformation is generally expressed as

$$x = Qx' + s \tag{1}$$

where x' is a position vector referring to a local coordinate and x is the corresponding position vector referring to the global coordinate. In this Note, lower- and upper-case boldface letters, respectively, denote vectors and matrices; the dashed variables are used to express that they refer to the local coordinate. The rotation matrix Q and translation vector s are defined between the coordinates, where $Q = Q(\theta)$ is an orthogonal matrix and actually expressed in terms of the rotation angle vector $\theta = [\psi, \theta, \phi]^T$. We adopt the roll-pitch-yaw angles for the rotation angle vector in this study; the Euler angles can also be available.[3] Coordinate transformation of a velocity vector is obtained as the time derivative of Eq. (1) as follows:

$$\dot{x} = \dot{Q}x' + Q\dot{x}' + \dot{s} \tag{2}$$

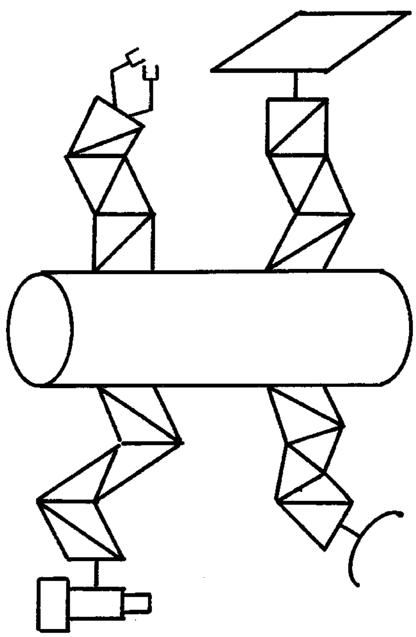

Fig. 1 Conceptual sketch of multiunit orbital platform system with VGTs for momentum interference reduction.

Received 24 May 2000; revision received 9 April 2001; accepted for publication 17 July 2001.

*Associate Professor, Department of Computer and Systems Engineering. Senior Member AIAA.

†Professor, Department of Computer and Systems Engineering.

where

$$\dot{\boldsymbol{Q}} = \frac{\partial \boldsymbol{Q}}{\partial \psi}\dot{\psi} + \frac{\partial \boldsymbol{Q}}{\partial \theta}\dot{\theta} + \frac{\partial \boldsymbol{Q}}{\partial \phi}\dot{\phi} \tag{3}$$

Transformation of Linear and Angular Momentum

Linear momentum $\boldsymbol{p}$, which occurs within a mission unit, is expressed as

$$\boldsymbol{p} = \int \rho \dot{\boldsymbol{x}} \,\mathrm{d}v \tag{4}$$

where ρ is the material density and $\mathrm{d}v$ is an infinitesimal volume element. Substituting Eq. (2) for $\dot{\boldsymbol{x}}$, the coordinate transformation of linear momentum is derived as

$$\boldsymbol{p} = \int \rho(\dot{\boldsymbol{Q}}\boldsymbol{x}' + \boldsymbol{Q}\dot{\boldsymbol{x}}' + \dot{\boldsymbol{s}})\,\mathrm{d}v = \dot{\boldsymbol{Q}}\boldsymbol{y}' + m\boldsymbol{Q}\boldsymbol{p}' + m\dot{\boldsymbol{s}} \tag{5}$$

where m is the total mass of the mission unit and $\boldsymbol{y}$ is its weighted mass center expressed as

$$\boldsymbol{y} = \int \rho \boldsymbol{x} \,\mathrm{d}v \tag{6}$$

whose coordinate transformation can also be performed similarly as

$$\boldsymbol{y} = \boldsymbol{Q}\boldsymbol{y}' + m\boldsymbol{s} \tag{7}$$

Angular momentum $\boldsymbol{h}$, which occurs within the mission unit, is expressed as

$$\boldsymbol{h} = \int \rho \boldsymbol{x} \times \dot{\boldsymbol{x}} \,\mathrm{d}v \tag{8}$$

Its coordinate transformation on the basis of Eqs. (1) and (2) cannot be performed immediately in this case because of the vector product operation. Introducing the vector function for a 3×3 matrix $\boldsymbol{D} = [d_{ij}]$

$$\boldsymbol{\omega}(\boldsymbol{D}) = [d_{23} - d_{32}, d_{31} - d_{13}, d_{12} - d_{21}]^T \tag{9}$$

a vector product can be expressed as

$$\boldsymbol{a} \times \boldsymbol{b} = \boldsymbol{\omega}(\boldsymbol{a}\boldsymbol{b}^T) \tag{10}$$

On the basis of the linearity of function $\boldsymbol{\omega}$, angular momentum (8) is rewritten as

$$\boldsymbol{h} = \int \rho \boldsymbol{x} \times \dot{\boldsymbol{x}} \,\mathrm{d}v = \int \rho \boldsymbol{\omega}(\boldsymbol{x}\dot{\boldsymbol{x}}^T)\,\mathrm{d}v = \boldsymbol{\omega}(\boldsymbol{B}) \tag{11}$$

where

$$\boldsymbol{B} = \int \rho \boldsymbol{x}\dot{\boldsymbol{x}}^T \,\mathrm{d}v \tag{12}$$

is an auxiliary variable. Accordingly, the coordinate transformation of angular momentum $\boldsymbol{h}$ resolves into coordinate transformation of corresponding auxiliary variable $\boldsymbol{B}$. Substituting Eqs. (1) and (2) for $\boldsymbol{x}$ and $\dot{\boldsymbol{x}}$ in Eq. (12), the coordinate transformation is then formulated as follows:

$$\begin{aligned}\boldsymbol{B} &= \int \rho(\boldsymbol{Q}\boldsymbol{x}' + \boldsymbol{s})(\dot{\boldsymbol{Q}}\boldsymbol{x}' + \boldsymbol{Q}\dot{\boldsymbol{x}}' + \dot{\boldsymbol{s}})^T \,\mathrm{d}v \\ &= \boldsymbol{Q}\boldsymbol{A}'\dot{\boldsymbol{Q}}^T + \boldsymbol{Q}\boldsymbol{B}'\boldsymbol{Q}^T + \boldsymbol{Q}\boldsymbol{y}'\dot{\boldsymbol{s}}^T + \boldsymbol{s}\boldsymbol{y}'^T\dot{\boldsymbol{Q}}^T + \boldsymbol{s}\boldsymbol{p}'^T\boldsymbol{Q}^T + m\boldsymbol{s}\dot{\boldsymbol{s}}^T\end{aligned} \tag{13}$$

where $\boldsymbol{A}$ is a kind of quadratic moment expressed as

$$\boldsymbol{A} = \int \rho \boldsymbol{x}\boldsymbol{x}^T \,\mathrm{d}v \tag{14}$$

and its coordinate transformation is similarly obtained as

$$\boldsymbol{A} = \boldsymbol{Q}\boldsymbol{A}'\boldsymbol{Q}^T + \boldsymbol{Q}\boldsymbol{y}'\boldsymbol{s}^T + \boldsymbol{s}\boldsymbol{y}'^T\boldsymbol{Q}^T + m\boldsymbol{s}\boldsymbol{s}^T \tag{15}$$

On the basis of the formulation, the mechanical variables required for coordinate transformation of linear and angular momentum are m, $\boldsymbol{p}$, $\boldsymbol{y}$, $\boldsymbol{A}$, and $\boldsymbol{B}$ for a mission unit, irrespective of the number of its constituent movable structural elements.

Motion Planning of VGT

Kinematic Relation

VGT[2] is a mechanical system that has a topology of statically determinate truss structure and a number of length-adjustable truss members as its actuators. The kinematic relation of VGT can be formulated as geometrical relationship between its workspace vector and member lengths.[4] In this study, the workspace vector of the VGT, $\boldsymbol{z} = [\boldsymbol{s}^T, \boldsymbol{\theta}^T]^T$, consists of the position $\boldsymbol{s}$ and orientation $\boldsymbol{\theta}$ of the peripheral end and is assumed to express the translation and rotation of the local coordinate of the mission unit. It can be related to the member lengths vector $\boldsymbol{l} = [l_1, \ldots, l_{N_l}]^T$ through the nodal positions $\boldsymbol{x} = [\boldsymbol{x}_1^T, \ldots, \boldsymbol{x}_{N_x}^T]^T$ in the following general form:

$$\boldsymbol{z} = \boldsymbol{z}^x[\boldsymbol{x}(\boldsymbol{l})] = \boldsymbol{z}^l(\boldsymbol{l}) \tag{16}$$

The velocity relation is immediately obtained as

$$\dot{\boldsymbol{z}} = \boldsymbol{J}^{zl}\dot{\boldsymbol{l}} \tag{17}$$

where

$$\boldsymbol{J}^{zl} = \boldsymbol{J}^{zx}\boldsymbol{J}^{xl}, \qquad \boldsymbol{J}^{zx} = \frac{\partial \boldsymbol{z}}{\partial \boldsymbol{x}}, \qquad \boldsymbol{J}^{xl} = \frac{\partial \boldsymbol{x}}{\partial \boldsymbol{l}} \tag{18}$$

are the Jacobian matrices.

Formulation of Mechanical Variables for Truss

In the case of VGT or other truss structures, the mechanical variables introduced in the preceding section are formulated as follows:

$$\boldsymbol{p}_T = \sum_{i=1}^{N_L} \boldsymbol{p}_i, \qquad \boldsymbol{p}_i = \frac{1}{2}m_i\left(\dot{\boldsymbol{x}}_{\alpha_i} + \dot{\boldsymbol{x}}_{\beta_i}\right) \tag{19}$$

$$\boldsymbol{y}_T = \sum_{i=1}^{N_L} \boldsymbol{y}_i, \qquad \boldsymbol{y}_i = \frac{1}{2}m_i\left(\boldsymbol{x}_{\alpha_i} + \boldsymbol{x}_{\beta_i}\right) \tag{20}$$

$$\boldsymbol{A}_T = \sum_{i=1}^{N_L} \boldsymbol{A}_i$$

$$\boldsymbol{A}_i = \frac{1}{3}m_i\boldsymbol{x}_{\alpha_i}\boldsymbol{x}_{\alpha_i}^T + \frac{1}{6}m_i\boldsymbol{x}_{\alpha_i}\boldsymbol{x}_{\beta_i}^T + \frac{1}{6}m_i\boldsymbol{x}_{\beta_i}\boldsymbol{x}_{\alpha_i}^T + \frac{1}{3}m_i\boldsymbol{x}_{\beta_i}\boldsymbol{x}_{\beta_i}^T \tag{21}$$

$$\boldsymbol{B}_T = \sum_{i=1}^{N_L} \boldsymbol{B}_i$$

$$\boldsymbol{B}_i = \frac{1}{3}m_i\boldsymbol{x}_{\alpha_i}\dot{\boldsymbol{x}}_{\alpha_i}^T + \frac{1}{6}m_i\boldsymbol{x}_{\alpha_i}\dot{\boldsymbol{x}}_{\beta_i}^T + \frac{1}{6}m_i\boldsymbol{x}_{\beta_i}\dot{\boldsymbol{x}}_{\alpha_i}^T + \frac{1}{3}m_i\boldsymbol{x}_{\beta_i}\dot{\boldsymbol{x}}_{\beta_i}^T \tag{22}$$

where m_i is the mass of ith member and $\boldsymbol{x}_{\alpha_i}$ and $\boldsymbol{x}_{\beta_i}$ are the nodal positions of the both ends of the ith member. Subscript T denotes that the variables are for VGT. Truss members are assumed to have uniform cross section in the formulation.

On the basis of Eqs. (11) and (22), the linear relation between the angular momentum and the nodal velocity can be obtained in the following form:

$$\boldsymbol{h}_T = \sum_{i=1}^{N_L} \boldsymbol{h}_i$$

$$\begin{aligned}\boldsymbol{h}_i = &\left[\frac{1}{3}m_i\boldsymbol{\Omega}\left(\boldsymbol{x}_{\alpha_i}\right) + \frac{1}{6}m_i\boldsymbol{\Omega}\left(\boldsymbol{x}_{\beta_i}\right)\right]\dot{\boldsymbol{x}}_{\alpha_i} \\ &+ \left[\frac{1}{3}m_i\boldsymbol{\Omega}\left(\boldsymbol{x}_{\beta_i}\right) + \frac{1}{6}m_i\boldsymbol{\Omega}\left(\boldsymbol{x}_{\alpha_i}\right)\right]\dot{\boldsymbol{x}}_{\beta_i}\end{aligned} \tag{23}$$

where $\boldsymbol{\Omega}(\boldsymbol{a})$ is the matrix function for a three-dimensional vector $\boldsymbol{a} = [a_1, a_2, a_3]^T$, expressed as

$$\boldsymbol{\Omega}(\boldsymbol{a}) = \begin{bmatrix} 0 & -a_3 & a_2 \\ a_3 & 0 & -a_1 \\ -a_2 & a_1 & 0 \end{bmatrix} \tag{24}$$

which satisfies the following relation:

$$\boldsymbol{a} \times \boldsymbol{b} = \boldsymbol{\omega}(\boldsymbol{a}\boldsymbol{b}^T) = \boldsymbol{\Omega}(\boldsymbol{a})\boldsymbol{b} \tag{25}$$

Paying attention to the linearity of Eqs. (19) and (23) about the nodal velocities, the following equation is obtained as a superposition of these equations:

$$\boldsymbol{p}_T^* = \begin{bmatrix} \boldsymbol{p}_T \\ \boldsymbol{h}_T \end{bmatrix} = \boldsymbol{C}^{px}\dot{\boldsymbol{x}} \tag{26}$$

where $\boldsymbol{C}^{px}$ is the resultant coefficient matrix.

Motion Planning for Momentum Interference Reduction

We introduce the following operation $[\,\cdot\,]_{\dot\theta}$ for a linear vector function of the time derivative of rotation matrix $\boldsymbol{f} = \boldsymbol{f}(\dot{\boldsymbol{Q}})$, defined as

$$[\boldsymbol{f}(\dot{\boldsymbol{Q}})]_{\dot\theta} = \left[\boldsymbol{f}\left(\frac{\partial \boldsymbol{Q}}{\partial \psi}\right), \boldsymbol{f}\left(\frac{\partial \boldsymbol{Q}}{\partial \theta}\right), \boldsymbol{f}\left(\frac{\partial \boldsymbol{Q}}{\partial \phi}\right)\right] \tag{27}$$

which results in the coefficient matrix between $\boldsymbol{f}$ and $\dot{\boldsymbol{\theta}}$ expressed as

$$\boldsymbol{f} = [\boldsymbol{f}(\dot{\boldsymbol{Q}})]_{\dot\theta}\dot{\boldsymbol{\theta}} \tag{28}$$

Referring to Eqs. (5), (11), and (13), the coordinate transformation of linear and angular momentum of the mission unit can be expressed in the following form by means of the operation:

$$\boldsymbol{p}_U = m_U\dot{\boldsymbol{s}} + [\dot{\boldsymbol{Q}}\boldsymbol{y}'_U]_{\dot\theta}\dot{\boldsymbol{\theta}} + m_U\boldsymbol{Q}\boldsymbol{p}'_U \tag{29}$$

$$\boldsymbol{h}_U = \boldsymbol{\Omega}(\boldsymbol{Q}\boldsymbol{y}'_U + m_U\boldsymbol{s})\dot{\boldsymbol{s}} + \left[\boldsymbol{\omega}\left(\boldsymbol{Q}\boldsymbol{A}'_U\dot{\boldsymbol{Q}}^T + \boldsymbol{s}\boldsymbol{y}'^T_U\dot{\boldsymbol{Q}}^T\right)\right]_{\dot\theta}\dot{\boldsymbol{\theta}} + \boldsymbol{\omega}\left(\boldsymbol{Q}\boldsymbol{B}'_U\boldsymbol{Q}^T + \boldsymbol{s}\boldsymbol{p}'^T_U\boldsymbol{Q}^T\right) \tag{30}$$

where subscript U denotes that the variables are for the mission unit. These two equations can be arranged as

$$\boldsymbol{p}_U^* = \begin{bmatrix} \boldsymbol{p}_U \\ \boldsymbol{h}_U \end{bmatrix} = \boldsymbol{C}^{pz}\dot{\boldsymbol{z}} + \boldsymbol{r}^* \tag{31}$$

with the following matrix and vector:

$$\boldsymbol{C}^{pz} = \begin{bmatrix} m_U & [\dot{\boldsymbol{Q}}\boldsymbol{y}'_U]_{\dot\theta} \\ \boldsymbol{\Omega}(\boldsymbol{Q}\boldsymbol{y}'_U + m_U\boldsymbol{s}) & \left[\boldsymbol{\omega}\left(\boldsymbol{Q}\boldsymbol{A}'_U\dot{\boldsymbol{Q}}^T + \boldsymbol{s}\boldsymbol{y}'^T_U\dot{\boldsymbol{Q}}^T\right)\right]_{\dot\theta} \end{bmatrix} \tag{32}$$

$$\boldsymbol{r}^* = \begin{bmatrix} m_U\boldsymbol{Q}\boldsymbol{p}'_U \\ \boldsymbol{\omega}\left(\boldsymbol{Q}\boldsymbol{B}'_U\boldsymbol{Q}^T + \boldsymbol{s}\boldsymbol{p}'^T_U\boldsymbol{Q}^T\right) \end{bmatrix} \tag{33}$$

From Eqs. (17), (18), (26), and (31) we formulate the following motion planning problem in terms of the member velocity $\dot{\boldsymbol{l}}$:

$$\begin{aligned} &\text{Find} && \dot{\boldsymbol{l}} \\ &\text{such that} && \begin{cases} \boldsymbol{J}^{zl}\dot{\boldsymbol{l}} = \dot{\underline{\boldsymbol{z}}} \\ (\boldsymbol{C}^{pz}\boldsymbol{J}^{zl} + \boldsymbol{C}^{px}\boldsymbol{J}^{xl})\dot{\boldsymbol{l}} = -\boldsymbol{r}^* \\ g(\dot{\boldsymbol{l}}) \rightarrow \text{Min} \end{cases} \end{aligned} \tag{34}$$

where $\dot{\underline{\boldsymbol{z}}}$ is the target workspace velocity to be achieved and $g(\dot{\boldsymbol{l}})$ is a criterion function adopted in order to resolve the kinematical redundancy. In the case of the criterion function $g(\dot{\boldsymbol{l}})$ in a quadratic form, the solution of the motion planning problem can be expressed as

$$\dot{\boldsymbol{l}} = \begin{bmatrix} \boldsymbol{J}^{zl} \\ \boldsymbol{C}^{pz}\boldsymbol{J}^{zl} + \boldsymbol{C}^{px}\boldsymbol{J}^{xl} \end{bmatrix}^+ \begin{bmatrix} \dot{\underline{\boldsymbol{z}}} \\ -\boldsymbol{r}^* \end{bmatrix} \tag{35}$$

by means of an appropriate generalized inverse[5] $[\,\cdot\,]^+$. In the following simulation study, we adopt the criterion expressed as

$$g = g(\dot{\boldsymbol{l}}) = \tfrac{1}{2}\dot{\boldsymbol{l}}^T\dot{\boldsymbol{l}} \tag{36}$$

which evaluates the magnitude of the VGT motion in member lengths; the motion planning problem is solved by means of the pseudo-inverse.

Computer Simulation

We conduct a computer simulation in order to demonstrate the effect of momentum interference reduction by means of the proposed motion planning. An antenna unit is assumed to be installed on the main structure of the platform system through a helical-mast-type VGT. It consists of 54 truss members, and the mass of each truss member is assumed to be 1 kg, that is, the total mass of the VGT is 54 kg. The mass of the antenna unit is assumed to be 10 kg. Figure 2a shows the initial posture of the VGT and antenna unit. The task to be performed by the VGT is to attain the target workspace $z^{\text{fin}} = [0.5, 0, 5.5\text{ m}; 0, 10, 0\text{ deg}]^T$ from the initial position $z^{\text{ini}} = [0, 0, 6\text{ m}; 0, 0, 0\text{ deg}]^T$ in 10 s while the antenna unit rotates 20 deg on the y axis of its own coordinate. The path in the workspace is assumed to be straight, and the velocity pattern minimizing total rate of acceleration is adopted. The time step for numerical integration and motion planning is 0.001 s. Figure 2b shows the resultant final posture achieved by means of the proposed momentum management approach. We also carry out another simulation of a VGT motion under the same task, which does not take account of momentum management. This corresponds to the motion planning (34) without the second constraint on momentum. The final posture in this case is shown in Fig. 2c. On the basis of the proposed motion planning approach, the maximum error in linear and angular momentum 5.3×10^{-3} kgm/s and 8.8×10^{-3} kgm^2/s is accomplished, while the maximum error becomes 4.5 kgm/s and 17 kgm^2/s for the motion without momentum consideration.

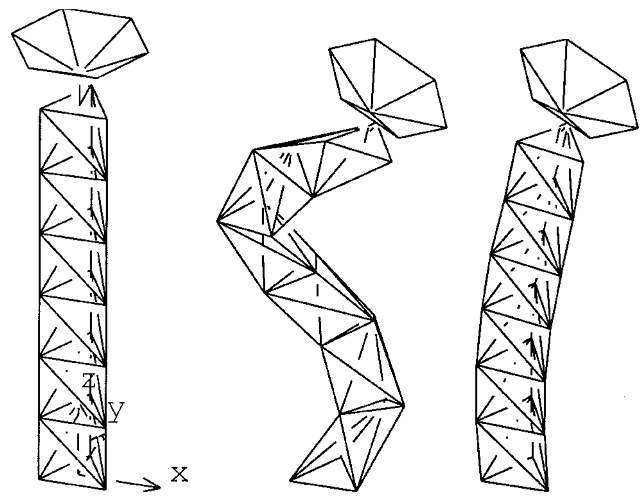

a) b) c)

Fig. 2 Computer simulation of VGT motion with antenna unit: a) initial posture, b) final posture obtained by the motion taking account of momentum management, and c) final posture obtained by a motion without taking account of momentum management.

Conclusions

Interference among mission units is considered to be one of the major problems for multiunit orbital platform systems. In the Note the interference caused by the conservation of momentum is studied, and an application of VGT for momentum management is presented. To deal with the local coordinate fixed to mission unit, we introduce a suitable formulation of coordinate transformation of linear and angular momentum. On the basis of the formulation, the criterion-oriented motion planning problem is developed, and a solution by means of generalized inverse is indicated. We also carry out a computer simulation, and the feasibility of the proposed approach is demonstrated.

Acknowledgment

This work was partially supported by the Ministry of Education, Science and Culture of Japan through Grant-in-Aid for Encouragement of Young Scientists 11750209.

References

[1]Wada, B. K., Fason, J. L., and Crawley, E. F., "Adaptive Structures," *Journal of Intelligent Material Systems and Structures*, Vol. 1, No. 2, 1990, pp. 157–174.

[2]Miura, K., Furuya, H., and Suzuki, K., "Variable Geometry Truss and Its Application to Deployable Truss and Space Crane Arm," *Acta Astronautica*, Vol. 12, No. 7/8, 1985, pp. 599–607.

[3]Paul, R. P., *Robot Manipulators: Mathematics, Programming, and Control*, MIT Press, Cambridge, MA, 1981, Chap. 2, pp. 41–63.

[4]Tanaka, M., Seguchi, Y., and Hanahara, K., "Kinematics of Adaptive Truss Permitting Nodal Offset (Configuration and Workspace Reach)," *Journal of Intelligent Material Systems and Structures*, Vol. 2, No. 3, 1991, pp. 301–327.

[5]Rao, C. R., and Mitra, S. K., *Generalized Inverse of Matrices and Its Applications*, Wiley, New York, 1971, Chap. 3, pp. 44–71.

A. M. Baz
Associate Editor

Modal Actuator/Sensor by Modulating Thickness of Piezoelectric Layers for Smart Plates

Dongchang Sun* and Liyong Tong†
University of Sydney,
Sydney, New South Wales 2006, Australia
and
Dajun Wang‡
Peking University,
100871 Beijing, People's Republic of China

I. Introduction

SMART structures with integrated distributed piezoelectric sensors and actuators have been extensively studied in recent years for their potential versatile applications in many aspects, such as aeronautical and astronautical engineering. The independent modal space control (IMSC),[1] which cannot be realized perfectly with the discrete sensors and actuators, can be implemented by the modal sensors and modal actuators with little observation and control spillover by using distributed piezoelectric wafers.[2–7] However, the modal actuators/sensors,[2–4] which are designed by shaping the electric pattern of the piezoelectric layers, are difficult to apply to two-dimensional structures, such as plates and shells, except some special cases. Although the distributed piezoelectric segment method[6,7] can be used for modal control of plates, it can lead to higher costs to control multiple modes simultaneously at a satisfied accuracy. Recently, Tzou et al.[8] gave generic ideas called "spatial thickness shaping" and "spatial surface shaping" to design the modal sensor for shell structures. However, all of their works are concentrated on the spatial surface method without discussing the spatial thickness shaping of the sensor layer.

In this Note, a new practical method is presented to design the modal sensors/actuators by means of modulating the thickness of the piezoelectric wafers. The modal actuators/sensors are designed to excite/sense the designated one or more modes by shaping the thickness of one piezoelectric layer. A simple control scheme is given to perform active control of the smart plates by a modal actuator and a modal sensor. The control energy can be made to be properly distributed on the dominant modes of the plate by the modal actuator and modal sensor, and, therefore, more effective control results can be achieved. Finally, two approaches are given for implementing the modal sensor/actuator approximately.

II. Basic Equations for the Piezoelectric Smart Plates

Consider the transverse vibration of a thin plate, on both surfaces of which two piezoelectric layers bonded as the distributed sensor and actuator, as shown in Fig. 1. Assume that the piezoelectric layers are much thinner than the host plate and they are perfectly bonded and that the bonding layers are so thin that their effects on the whole plate can be neglected.

The charge output of the sensor layer can be derived as

$$q(t) = -\iint_S F_s(x, y)\left(\frac{\partial^2 w}{\partial x^2} + \frac{\partial^2 w}{\partial y^2}\right) \mathrm{d}x\,\mathrm{d}y \tag{1}$$

where $q(t)$ is the charge output generated by the piezoelectric sensor layer, $w(x, y, t)$ is the transverse displacement of the smart plate, S is the area covered by the sensor layer, and $F_s(x, y) = e_{31}^s(x, y) r_s(x, y)$ is the spatial distribution function of the sensor layer in which $e_{31}^s(x, y)$ is the piezoelectric stress coefficient, $r_s(x, y)$ stands for the z coordinate of the midplane of the sensor layer from the neutral plane of the smart plate, that is, $r_s(x, y) = (z_0 + z_1)/2$ and z_0, z_1, z_2, and z_3 are z coordinates as shown in Fig. 1.

The differential equation of motion of the smart plate can be derived as

$$\rho h \frac{\partial^2 w}{\partial t^2} + \nabla^2(D\nabla^2 w) = -\nabla^2[F_a(x, y)V(x, y, t)] \tag{2}$$

where ρh is the equivalent mass density in unit area of the plate, $D(x, y)$ is the equivalent bending stiffness of the plate, V is the control voltage, and $F_a(x, y) = e_{31}^a(x, y) r_a(x, y)$ is the spatial distribution function of the actuator layer. Again, $e_{31}^a(x, y)$ is the piezoelectric stress coefficient, and $r_a(x, y) = (z_2 + z_3)/2$ is the z coordinate of the midplane of the actuator layer.

III. Modal Actuator Design

Consider the case that the voltage applied on the actuator layer is distributed uniformly in space. In this case the control voltage is only a time-dependent function, that is, $V(x, y, t) = V(t)$. The transverse displacement $w(x, y, t)$ can be expressed as a linear superposition of the modes of the plate, that is,

$$w(x, y, t) = \sum_{i=1}^{\infty}\sum_{j=1}^{\infty} \eta_{ij}(t) W_{ij}(x, y) \tag{3}$$

where $\eta_{ij}(t)$ and $W_{ij}(x, y)$ are the ijth modal coordinates and modal shape function. Substituting Eq. (3) into Eq. (2), we have

$$\ddot{\eta}_{ij}(t) + \omega_{ij}^2 \eta_{ij}(t) = -V(t) \iint_S \nabla^2[F_a(x, y)] W_{ij}(x, y)\, \mathrm{d}x\,\mathrm{d}y \qquad i, j = 1, 2, \ldots, \infty \tag{4}$$

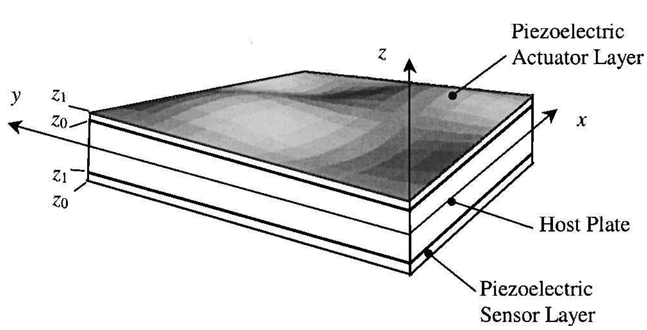

Fig. 1 Plate with piezoelectric sensor and actuator layer.

Received 8 November 1999; revision received 20 April 2001; accepted for publication 17 July 2001.

*Research Associate, School of Aerospace, Mechanical and Mechatronic Engineering; on leave, Associate Professor, School of Mechanical Engineering, Hebei University of Technology, Tianjin 300130, People's Republic of China.

†Associate Professor, School of Aerospace, Mechanical and Mechatronic Engineering. Senior Member AIAA.

‡Professor, Department of Mechanics and Engineering Science.